Am J Transl Res 2024;16(5):2011-2023
www.ajtr.org /ISSN:1943-8141/AJTR0154756

Original Article

Metal copper and silver revealed potent antimicrobial activity for treating *Caenorhabditis elegans* infected with *carbapenemase-producing Klebsiella pneumonia*

Ling Cao, Lili Tan, Liping Li

Department of Clinical Laboratory, The Third Affiliated Hospital of Nanchang University (The First Hospital of Nanchang), Nanchang 330008, Jiangxi, P. R. China

Received December 4, 2023; Accepted May 6, 2024; Epub May 15, 2024; Published May 30, 2024

Abstract: Objectives: The increasing issue of bacterial resistance, coupled with inadequate progress in developing new antibiotics, necessitates exploring alternative treatments. Antibacterial biomaterials, such as silver and copper, possess advantageous properties such as heat resistance, durability, continuity, and safety. Particularly, they can effectively eliminate pathogenic bacteria while preserving cellular integrity, emphasizing the necessity of identifying optimal metal ion concentrations for practical application. *Caenorhabditis elegans* (*C. elegans*) can serve as a noteworthy model in this context. This study employed a *C. elegans* infection model to assess the efficacy of antibacterial metal ions. Methods: Hematoxylin-eosin (HE) staining and inductively coupled plasma mass spectrometry (ICP-MS) assay were utilized to determine the toxic levels of metal ions in mice. Additionally, RNA sequencing (RNA-seq) and assessment of reactive oxygen species (ROS) production in the *C. elegans* model were conducted to elucidate the mechanisms underlying metal ion toxicity. Results: Silver ion concentrations ranging from 10^{-6} to 10^{-7} M and copper ion concentrations ranging from 10^{-4} to 10^{-5} M exhibited antimicrobial properties without eliciting cytotoxic effects. Analysis of the transcriptome data derived from mRNA isolated from *C. elegans* indicated that CRKP infection activated the FoxO signaling pathway, potentially leading to ROS accumulation and *C. elegans* demise. Conclusions: In conclusion, *C. elegans* serves as a comprehensive infection model for assessing antibacterial metal ions.

Keywords: Caenorhabditis elegans, metal ion, anti-infective agents

Introduction

The World Health Organization (WHO) has declared that carbapenem-resistant (CR) bacteria present a major concern for public health [1]. The increasing prevalence of antibiotic resistance and the few number of novel antibiotics have limited the available treatment choices for bacterial infections. Consequently, there is an urgent need to investigate alternative antibiotics. Metal ions have emerged as potential candidates due to their distinct antibacterial properties compared to conventional antibiotics [2]. Silver and copper in particular have gained significant attention as antibacterial biomaterials due to several advantages [3, 4]. The correlation between the antibacterial property and cytotoxicity of metal ions exhibits substantial variability, and the precise mechanisms underlying the antimicrobial property of metal ions remain inadequately elucidated [5-7]. Previous studies have demonstrated that small quantities of silver and copper bring advantages to human health while exerting detrimental effects on microbes. In fact, silver possesses potent antibacterial properties with minimal toxicity for human cells [8]. Notably, there is a growing interest in using copper as an antimicrobial substance [9]. For instance, copper salts have been integrated into mouthwashes and toothpastes as antimicrobial agents for managing gingivitis [10]. Currently, studies on metal ions primarily focus on the correlation between their antibacterial characteristics and cytotoxicity; however, there is less reliance on the results of in vitro experiments. In vitro plate colony-counting approach cannot account for the effect of in vivo interactions. Consequently, the use of innocuous metal compounds has been limited due to potential safety issues.

https://doi.org/10.62347/DIE08870

Mammalian models are both expensive and time-intensive [11, 12]. Rodent models demonstrate a predictive accuracy of approximately 50% when predicting specific toxic effects on humans [13-15]. Recently, growing research indicated that C. elegans offers valuable platforms for measuring the pathogenesis of microbial infection and host reactions to intracellular infection.

The present study explored the efficacy of different concentrations of metal ions in combating CRKP, utilizing a comprehensive C. elegans screening system. Furthermore, the potential cytotoxic effects of these antibacterial metal ions were examined by assessing the survival rate and observed behavior of C. elegans at different concentrations. The primary objective of this study was to understand the changes in host gene expression patterns after infection with CRKP in C. elegans. Additionally, we investigated the mechanisms associated with CRKP infection and established a model for screening anti-infective drugs. Our findings shed light on the host's response to Klebsiella pneumonia infection and provide valuable insight into the broader context of antimicrobial defense in C. elegans.

Materials and methods

General materials

Silver nitrate ($AgNO_3$, BioReagent grade) and copper chloride ($CuCl_2.2H_2O$, BioReagent grade) were purchased from Sigma-Aldrich (St. Louis, MO, USA), and serial dilutions in purified water were prepared to prevent silver salt precipitation. The solution of antibacterial metal ions was prepared and filtered using a sterile, single-use 0.22 μm filter (Millex-GS, Millipore, France). Carbapenem-resistant *Klebsiella pneumoniae* (CRKP) was obtained from the Guangzhou General Hospital of Guangzhou Military Command of PLA (Guangzhou, People's Republic of China).

C. elegans and culture conditions

The *C. elegans* glp-4(bn2);sek-1 (km4) was used because the glp-4 mutation makes *C. elegans* incapable of producing progeny at 25°C, and sek-1 mutant animals are relatively immunocompromised, which decreased the duration of the assay [16, 17]. The *C. elegans* strain was propagated on a nematode growth medium (NGM) and fed on the standard laboratory food source, *E. coli* OP50. The animals were age-synchronized by bleaching with alkaline hypochlorite and sodium hydroxide to liberate embryos. Embryos were placed into plates containing concentrated *E. coli* OP50 at 25°C until the worms reached the young adult stage.

Lethality test based on the C. elegans model

Lethality tests were conducted on the synchronized young adult nematode exposed to different concentrations of Ag^+ and Cu^{2+} [18]. Briefly, each test consisted of seven concentrations and a control. 20 ± 1 young adult *C. elegans* were transferred to 96-well plates containing 200 μL of the test solution in each well. The plate was incubated at 25°C and survival was monitored every 24 h following exposure to the metal ion.

Lethality test of Ag^+ and Cu^{2+} in the mouse model

Animal studies were conducted at the Guangzhou General Hospital of Guangzhou Military Command (Guangzhou, Guangdong, China). Animals received humane care throughout the experiment, and all procedures were approved by the Guangzhou General Hospital of Guangzhou Military Command. Kunming mice were purchased from Southern Medical University Laboratory Animal Center (Guangzhou, Guangdong, China) and were allowed to acclimatize to the animal room conditions for two weeks before the study. In total, 42 mice were randomly divided into 7 groups of 6 animals each (3 males and 3 females per group). Three concentrations of silver ions and copper ions were selected, based on the toxicity results from the nematode-lethality test. Three mouse groups were injected with different concentrations of Ag^+ (10^{-4} M, 10^{-5} M, and 10^{-6} M), and the remaining three groups of mice were injected with different concentrations of Cu^{2+} (10^{-2} M, 10^{-3} M, and 10^{-4} M). Sterile water was injected into the control group. A single dose of 50 ml/kg was administered. Animals were injected once per week for 9 weeks. The environmental conditions were set at a temperature of 22 ± 2°C and a relative humidity of 55 ± 15%, with air circulation and 12 h light/dark cycle. The mice had free access to standard diet and tap water ad libitum during the experi-

ment. The animals were monitored for gross behavioral, neurologic, autonomic, and toxic effects for the first 24 h and then daily for 14 days. Toxic effects were assessed based on mortality. All experimental mice were euthanized with carbon dioxide. The euthanasia was performed with carbon dioxide inhalation at a flow of 61/min [19].

Tissue collection

During necropsy, organs and tissues were assessed for gross visible lesions, and tissues and organs were preserved in 10% neutral buffered formalin (NBF). Livers and kidneys were collected for histopathology. In addition, livers were stored at -80°C for total silver and copper analysis by ICP-MS. The preserved organs and tissues of animals from the control and ion groups were subjected to histological examination. The organs were fixed in a 10% solution of buffered formalin (pH = 7.4) and embedded in paraffin for histopathological examination. 5 μm sections of each tissue were stained with HE. Each section was observed under an Olympus BX-51 microscope (Olympus, Tokyo, Japan). Tissues in 1 ml fixative were stored in 10 ml of 70% nitric acid overnight to start the digestion process. Samples were then microwave-digested in an Xpress microwave digester (CEM Corp., Matthews, NC, USA). The temperature was ramped to 200°C and maintained at this temperature for 20 minutes. Samples were subsequently boiled down to less than 1 ml each and reconstituted in water to reach exactly 10 ml volume. Ag^+ and Cu^{2+} levels in liver tissues were measured using a 7700 Series ICP-MS from Agilent Technologies (Santa Clara, CA). Each time point represented the average from at least three individual mice.

Screening antibacterial ion concentration based on the C. elegans infection model

Overnight cultures of *K. pneumonia*/CRKP were grown in BHI broth and centrifuged to pellet the bacteria. The pellet was suspended in a medium composed of 20% BHI, 80% M9 buffer, and 5.0 $\mu g.ml^{-1}$ nalidixic acid to prepare a suspension of 10^6 cells per ml (OD_{600} = 0.03). Nalidixic acid was used to inhibit *E. coli* growth as it did not affect other bacteria. Subsequently, the bacterial suspension was transferred to a centrifuge tube containing synchronized young adult nematodes for 12 h. The infected worms were then washed with a medium until the solution was clear. For the antibacterial ion screening assay, a 96-well plate was filled with 20 infected *C. elegans* per well. Wells containing uninfected *C. elegans* served as blank controls. The concentrations of silver (Ag^+) and copper ions (Cu^{2+}) varied from 10^{-2} M to 10^{-7} M. They were transferred to wells to generate multiple concentrations for antibacterial treatment. Purified water served as the negative control. After 12 h, the plate was observed under a stereo-microscope to score worm survival. For each treatment, 60 *C. elegans* were transferred to three wells (20 per well), representing three technical replicates. 1 μg/ml tigecycline (Aladdin) dissolved in ddH_2O was used as positive and negative controls.

RNA extraction, library construction, and sequencing

C. elegans were cultured for 0, 6, 12, or 24 hours with Klebsiella pneumonia (OD_{600} = 0.03). Uninfected *C. elegans* were synchronized by standard bleach treatment. After bleaching, animals (L4 stage) were inoculated with *Klebsiella pneumonia* (OD_{600} = 0.03). Animals were rinsed off from the tubes, the supernatant was removed after centrifugation, and 1 ml of Trizol was added. Total RNA was extracted using Trizol and mRNA was subsequently enriched using OligoTex mRNA mini (Qiagen) according to the manufacturer's protocol. RNA quality and quantity were assessed on an Agilent 2100 Bioanalyzer (Agilent Technologies, Palo Alto, CA, USA) and confirmed using RNase-free agarose gel electrophoresis. The RNA from the three replications was pooled, and enriched by Oligo (dT) beads. Microanalysis for each treatment was performed in biological triplicates. For transcriptomic analyses, *C. elegans* infected with *Klebsiella pneumonia* (0, 6, 12, or 24 hours) were defined as CK, T1, T2, and T3, respectively. Subsequently, the enriched mRNAs were fragmented using a fragmentation buffer and reverse transcribed into cDNA with random primers. Second-strand cDNA was synthesized using DNA polymerase I, RNase H, dNTPs, and buffer. cDNA fragments were purified using a Qiaquick PCR extraction kit (Qiagen, Venlo, The Netherlands), end-repaired, poly(A) added, and ligated to Illumina sequencing adapters. The ligation products were size selected using agarose gel electro-

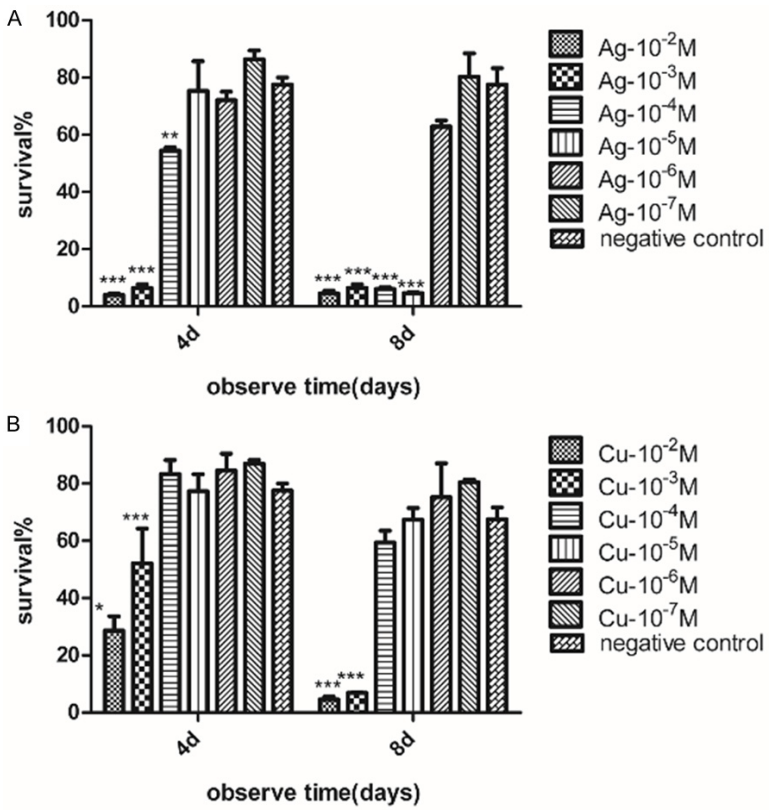

Figure 1. Percent survival of *C. elegans* 4 days post exposure to metal ions. A. 10^{-2}-10^{-7} M Ag^{+}; B. 10^{-2}-10^{-7} M Cu^{2+}. Data represent 3 replicate experiments, with each experiment containing 3 replicate wells. $P < 0.05$ for significance of interaction term in 2-factor ANOVA, $*P < 0.05$, $**P < 0.01$, $***P < 0.01$.

phoresis, PCR amplified, and sequenced using Illumina HiSeq2500 (Gene Sagene Biotech, Guangzhou, China).

ROS level determination

The toxic mechanisms of silver and copper ions were investigated using a ROS assay to understand better the toxic properties of metal ions. ROS were quantified as described previously [20]. *C. elegans* treated with the metal ions for 24 h were washed twice with ddH_2O and once with M9 media. *C. elegans* were then placed into M9 media mixed with dichlorofluorescein (DCF) at 25°C for 30 min. ROS detection was conducted using a BX-51 microplate reader (Olympus, Tokyo, Japan) at an excitation wavelength of 528 nm and emission at 485 nm. All measurements were performed in the dark.

Statistical analysis

Statistical analysis was performed with SPSS version 16.0 software (version 16.0, SPSS Inc., Chicago, IL, USA) and Graphpad PRISM software (GraphPad Software Inc., San Diego, CA). The survival analysis used Log-rank (Mantel-Cox) test. Data was analyzed using Student's t-test. The data are presented as the mean + SD, and significant statistical differences are presented as asterisks ($*P \leq 0.05$; $**P \leq 0.01$; $***P \leq 0.001$). All experiments about C. elegans experiments presented were repeated at least three times. In addition, the animal experiments were conducted in parallel with three mice.

Results

The cytotoxic effects of Ag^{+} and Cu^{2+} ions in a C. elegans model

The survival rates of *C. elegans* 4 days (4d-LC_{50}s) and 8 days (8d-LC_{50}s) after exposure to different concentrations of Ag^{+} and Cu^{2+} were estimated based on a *C. elegans* lethality test. The results indicated that the survival rate increased with decreasing Ag^{+} or Cu^{2+} concentrations. The results indicated that 10^{-6}-10^{-7} M of Ag^{+} and 10^{-4}-10^{-7} M of Cu^{2+} were non-toxic to *C. elegans* (**Figure 1**).

Lethality test of Ag^{+} and Cu^{2+} using the mouse model

To confirm the non-lethal concentrations of Ag^{+} and Cu^{2+}, mice treated with 10^{-4}-10^{-6} M of Ag^{+} or 10^{-2}-10^{-4} M of Cu^{2+} were followed for 9 weeks. The results showed that treatment with 10^{-4}-10^{-6} M of Ag^{+} did not lead to death (**Figure 2A**). In contrast, the 21-day mortality rate of mice exposed to 10^{-2} M Cu^{2+} was 100%, and that of mice exposed to 10^{-3} M of Cu^{2+} was 34%. HE staining of mouse liver tissue was used to detect the toxicity of metal ions to mice organs. Liver tissues were damaged in animals treated with 10^{-4}-10^{-5} M of Ag^{+} and 10^{-2}-10^{-3} M of Cu^{2+} (**Figure 2B**). Mice treated with 10^{-2}-10^{-3} M of Cu^{2+} suffered from diffuse and severe midzone hepatocellular necrosis, hemorrhage, and lym-

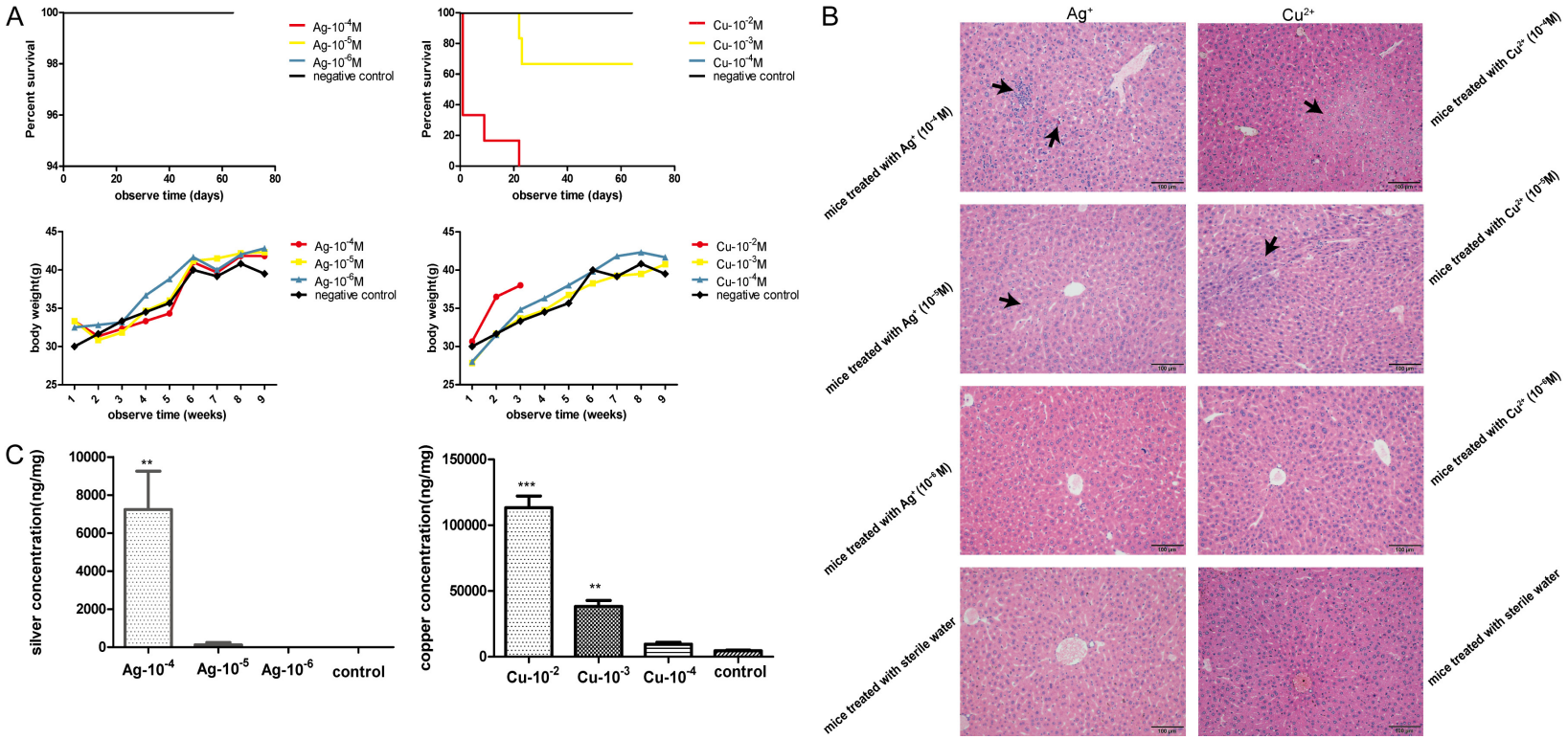

Figure 2. Lethality test of Ag^{+} and Cu^{2+} using the mouse model. A. The survival curve and body weight growth curves during the 9-week administration by injection with Ag^{+} and Cu^{2+}. Plotted values are mean treatment body weights for 9 weeks; B. Histological changes in mice liver after inject administration of Ag^{+} and Cu^{2+}; C. Silver tissue concentration after intraperitoneal injection administration of Ag^{+}, Cu^{2+} in mice. Data were expressed as means ± SD. Statistical significance: $^{**}P < 0.01$, $^{***}P < 0.001$.

phocyte infiltration in the hepatic portal space, necrosis, and scattered hemorrhages. Mice injected with 10^{-4} M of Ag^{+} exhibited perivascular edema, lymphocyte infiltration, and necrosis in the hepatic portal space. Mice treated with 10^{-5} M of Ag^{+} had only mild lymphocyte infiltration and necrosis in the hepatic portal space. Hepatic lesions were not observed and lymphocyte infiltration decreased in mice treated with 10^{-6} M of Ag^{+} and 10^{-5} M of Cu^{2+}. Animals treated with low concentrations had only focal and mild inflammation in their liver tissues. The concentrations of the Ag^{+} and Cu^{2+} in mice liver tissues were determined using ICP-MS (**Figure 2C**). The mean concentration of Cu^{2+} was 4600 ng/g for the control group over the study, but the total Ag^{+} levels for each control formulation were less than the ICP-MS limit of quantitation (260 ng/g) throughout the study. There was no significant difference in the mean concentration of Ag^{+} in mouse liver tissues between 10^{-5} M or 10^{-6} M Ag^{+} treatment groups ($P > 0.05$). However, the average concentration of Cu^{2+} in the liver tissues of mice was significantly different between 10^{-2} M and 10^{-3} M Cu^{2+} treatment groups ($P < 0.05$). These results showed that 10^{-6}-10^{-7} M of Ag^{+} and 10^{-4}-10^{-7} M of Cu^{2+} were not toxic.

The antibacterial effect of Ag^{+} and Cu^{2+} ions in the C. elegans infection model

A 12-hour treatment cycle with Ag^{+} or Cu^{2+} was conducted to assess the antibacterial efficacy of Ag^{+} and Cu^{2+} against CRKP infection of *C. Elegans*. The screening procedure was aided by noticeable disparities in the physical characteristics between live and dead worms. Infected worms generally exhibited reduced size compared to healthy worms nourished with E. coli OP50. Deceased worms were immobile, lacked muscle tonicity, and were unresponsive to external stimuli.

In the medium, *C. elegans* exhibited a straight rigid rod-like appearance and lacked observable pharyngeal pumping. Conversely, worms exposed to E. coli OP50 displayed a sinusoidal 'S' shape and exhibited active movement. These *C. elegans* experienced growth and eventually evolved into gravid adults (**Figure 3A**). The interaction between *C. elegans* and CRKP during infection is a multifaceted and dynamic process. The activity of *C. elegans* decreased after 6 hours of infection, followed by a subsequent decline in autonomous activity after 12 hours of infection, accompanied by observable pharyngeal pumping. 24 hours after the infection, the intestines of *C. elegans* were filled with a significant quantity of bacteria, neutralizing independent activities. Approximately one hour later, oropharyngeal activity was decreased (**Figure 3B**). To construct the infection model, we chose an infection time of 12 hours and an infection concentration of 1.5×10^{6} cfu/ml CRKP [21, 22]. The survival rates of *C. elegans* infected with CRKP significantly increased after treatment with 10^{-2} M to 10^{-7} M concentrations of Ag^{+} and Cu^{2+} for 12 h. After treatment, over 50% of *C. elegans* survived, compared to approximately 20% survival rate observed in the untreated control group. The control group, consisting of *C. elegans* fed on E. coli OP50, remained alive throughout the entire experiment. Our findings revealed that 12 h treatment with Ag^{+} exhibited antimicrobial properties within the concentration range of 10^{-2}-10^{-6} M. Utilizing the identical analytical approach, the antimicrobial concentration range of Cu^{2+} ions was determined to be 10^{-2}-10^{-4} M (**Figure 3C**). Combined with previous cytotoxicity results, it was established that 10^{-6} M of Ag^{+} and 10^{-4} M of Cu^{2+} can exhibit antimicrobial activity without any cytotoxic effects.

Differential gene expression pattern analysis, clustering, and functional enrichment in C. elegans infected with CRKP

The transcriptome data of mRNA isolated from *C. elegans* infected with CRKP were analyzed to uncover the pathogenesis of CRKP infection in *C. elegans* and provide helpful information for selecting and designing antimicrobial agents. The transcriptome data were generated from the mRNA isolated from *C. elegans* infected with CRKP (OD_{600} = 0.03) for 0 h, 6 h, 12 h, and 24 h. Following 6 hours of infection, 1899 genes were downregulated, while 1321 genes were upregulated. After 12 hours of infection, 856 genes were upregulated and 823 genes were downregulated. 24 hours after the fatal infection, 1077 genes were upregulated, and 1021 genes were downregulated (**Figure 4A**). Gene ontology (GO) analysis of differentially expressed genes at various infection time points revealed a predominant enrichment of these genes during anatomical structure de-

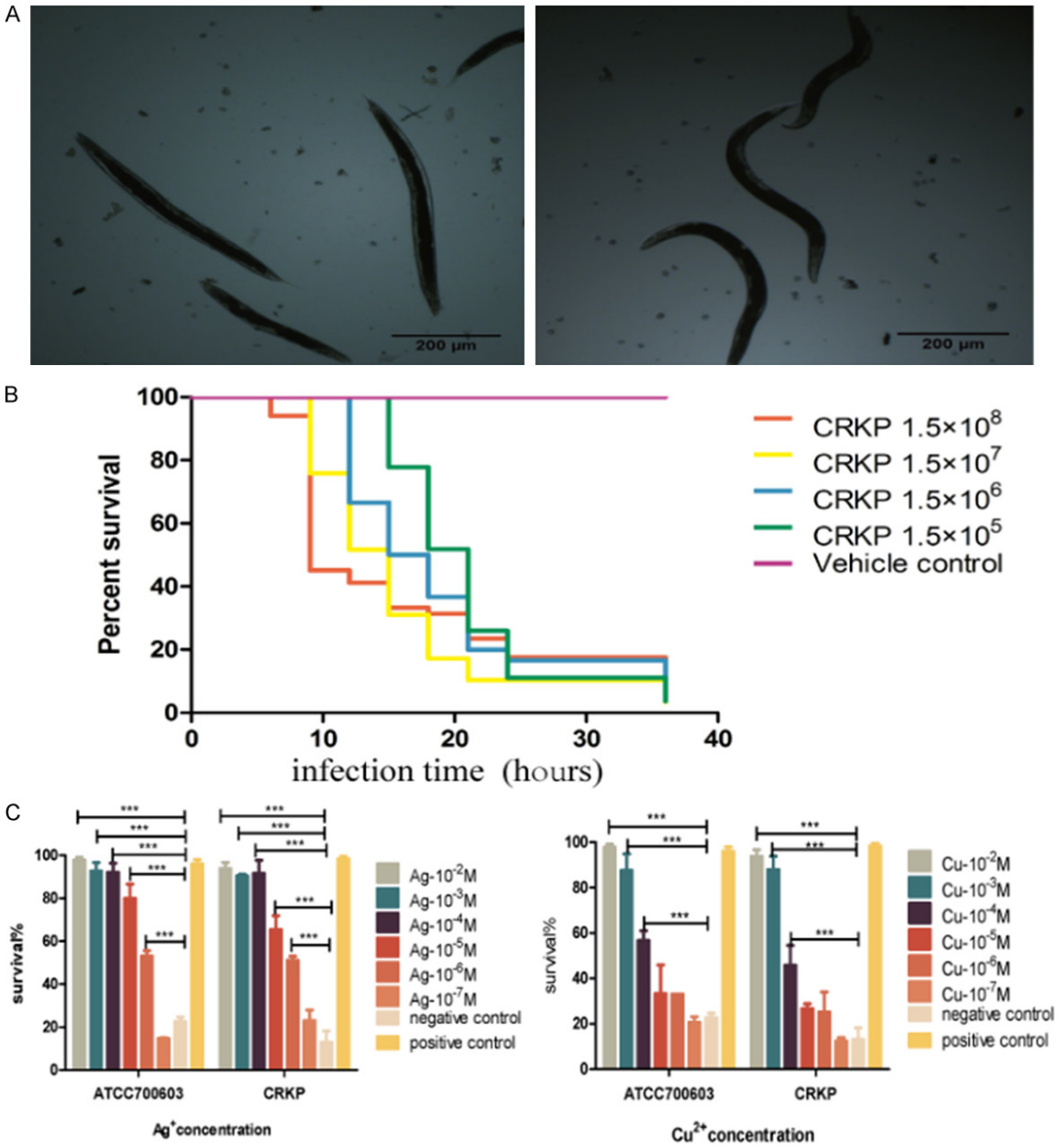

Figure 3. The antibacterial effect of Ag^+ and Cu^{2+} ions in CRKP infected *C. Elegans*. A. Distinct appearances of dead (*C. elegans* exposed either to CRKP) and alive (*C. elegans* exposed either to E. coli OP50); B. Survival curves of CRKP infected *C. elegans* at different concentrations, Log-rank (Mantel-Cox) test was performed for survival analysis using Graph Pad Software, $P < 0.001$; C. The survival rate against ATCC700603/CRKP (right) infected *C. elegans* in the presence of metal ions at different concentrations. The bacteria concentration was 10^6 CFU/ml. Data are presented as the mean ± standard deviation. Significant difference of antibacterial rate was observed with respect to the experiment groups with negative control (ddH_2O) (n = 3, $***P < 0.001$).

velopment, cell cycle, cell differentiation, chromosome organization, cytoskeleton organization, developmental process, mitosis, organelle organization, reproduction, single-organism developmental process, small molecule metabolism, cytoskeleton, extracellular matrix, macromolecular complex, nuclear chromosome, protein complex, and oxidoreductase activity (**Figure 4B**). The KEGG enrichment analysis of differentially expressed genes revealed enrichment in various pathways, including DNA replication, calcium signaling pathway, and FoxO


A
DiffExp Gene Statistics
UP
DOWN
CK-vs-T3
CK-vs-T2
CK-vs-T1
1021
1077
823
856
1899
1321
0
500
1000
1500
2000
2500
Number of Genes
B
Level2 GO terms of CK-vs-T1
Level2 GO terms of CK-vs-T2
Level2 GO terms of CK-vs-T3
Num of Genes
up
down
biological_process
cellular_component
molecular_function
C
Top 20 of Pathway Enrichment
Pyrimidine metabolism
Caffeine metabolism
Cysteine and methionine metabolism
Biosynthesis of amino acids
Nitrogen metabolism
Drug metabolism − other enzymes
Phagosome
Linoleic acid metabolism
Calcium signaling pathway
Arginine and proline metabolism
Mismatch repair
Butanoate metabolism
beta−Alanine metabolism
Valine, leucine and isoleucine degradation
FoxO signaling pathway
Alanine, aspartate and glutamate metabolism
Glyoxylate and dicarboxylate metabolism
ABC transporters
Glycine, serine and threonine metabolism
DNA replication
Pathway
RichFactor
PValue
GeneNumber

Figure 4. Transcriptional analysis of differentially expressed genes in *C. Elegans* infected with CRKP. A. Number of differentially expressed genes at different time points post-infection; B. Functional analysis of differentially expressed genes in Caenorhabditis elegans at each time point after CRKP infection performed using Gene Ontology (GO) classification; C. Enrichment analysis of KEGG pathways associated with differentially expressed genes in *C. elegans* infected with CRKP at 12 H.

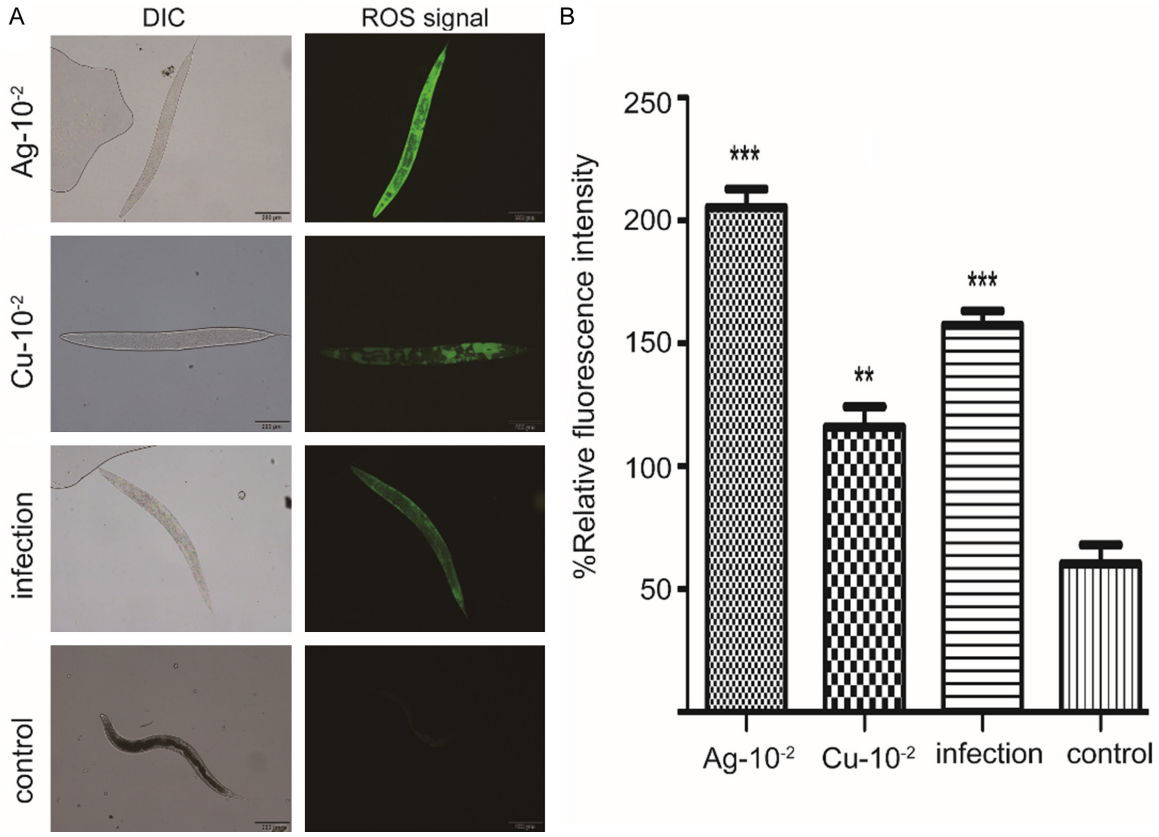

Figure 5. Measurement of ROS levels in nematodes infected with lethal and toxic strains. A. The confocal laser scanning micrographs showing the ROS production in nematodes exposed to silver ions, copper ions and K. pneumonia by DCFH-DA staining method; B. Fluorescence intensity of each group calculated using Image J software (**P < 0.01, ***P < 0.001).

signaling pathway (**Figure 4C**). The FoxO pathway is known to exert multifaceted and significant effects on cellular processes, such as proliferation, cell cycle arrest, anti-oxidant defense, and apoptosis induction at 24 h post-infection. Further analysis of genes from the FoxO signaling pathway unveiled that cyb-1, cyb-3, lgg-3, plk-1, plk-2, plk-3, ctl-3, prmt-1, and skpt-1 genes were downregulated, weakening the antioxidant response and inducing oxidative stress [23, 24].

Measurement of ROS content in C. elegans exposed to ion metals or CRKP

Transcriptome data analysis revealed that *C. elegans* death after infection with CRKP was linked to decreased expression of genes related to the FoxO signaling pathway and subsequent increase in ROS levels. We measured the ROS content of infected *C. elegans* after exposure to toxic concentrations of Ag^{+} and Cu^{2+} to verify how infection led to *C. elegans* death. The results showed that compared to the control group, ROS production was significantly increased in organisms exposed to metal ions. Acute exposure to Ag^{+} and Cu^{2+} at lethal concentrations increased ROS production (**Figure 5**). Numerous in vivo and in vitro nanotoxicology studies have indicated that free radical generation is the major mechanism of toxicity, which subsequently leads to oxidative stress, DNA damage, cytotoxicity, apoptosis, and tumorigenesis [25-27]. Hence, ROS production

appears to be the major contributor to worm death after exposure to metal ions and CRKP. Additionally, studies have indicated that reducing ROS levels with proper antioxidants may be a useful strategy to prevent or delay these pathologic processes [28, 29]. Therefore, antioxidants might protect against metal ion toxicity and ROS-mediated damage after CRKP infection. Antioxidants can attenuate metal ion toxicity but maintain their antibacterial action, which is expected to become a new direction of antimicrobial drug research and development in the future.

Discussion

The preliminary phases of screening antimicrobial ions commonly include in vitro techniques that emphasize direct bacteriostatic or bactericidal effects. Nonetheless, the application of these techniques in assessing compounds with unique mechanisms of action is limited due to various factors [30, 31]. Culturing specific microorganisms under viable conditions can be challenging. Furthermore, increased concentrations of compounds used for in vitro screening may exhibit toxicity or suboptimal pharmacokinetic characteristics in subsequent developmental stages. In the past decade, antimicrobial drug discovery has shifted toward using whole animal models, like zebrafish and C. elegans, to screen new compounds and uncover their mechanisms of action [32]. C. elegans model can help assess direct antimicrobial effects and potential immune mechanisms involved in antimicrobial effects. Using a whole live animal model, like C. elegans, can provide important information on systemic toxicity of compounds in the early stages of drug discovery [33]. The self-fertilization and genetic homogeneity of C. elegans make it a valuable model for studying the effects of novel compounds. Inbreeding mutant strains of C. elegans from a homogeneous genetic background can help investigate the mechanism of new compounds, making it an ideal organism that links in vitro assays to vertebrate models. C. elegans is a useful tool for discovering new antimicrobial drugs. It can be fatally infected by various human pathogens, such as *Staphylococcus aureus* [34], *Serratia marcescens* [35], *Pseudomonas* aeruginosa [36], Klebsiella pneumoniae, Enterococcus faecalis, and Candida albicans [37]. In this study, a C. elegans model of CRKP infection was established and used to measure the antibacterial effects of metal ions. Co-cultivating C. elegans with 10^{-6}-10^{-7} M silver ions and 10^{-4}-10^{-5} M copper ions showed antimicrobial effects without harming host cells. This supports previous studies that focused on in vitro and cellular tests [38, 39]. Animal models were then used to confirm the safety of these metal ions.

Silver ions at 10^{-4} M to 10^{-6} M did not affect mouse survival and did not lead to liver damage at 10^{-4} M to 10^{-5} M [40]. Animal models were used to confirm the effects of different concentrations of copper ions on mouse survival. Lower concentrations of silver and copper ions were non-toxic to nematodes and mice. Copper ions at different concentrations were administered to mice, showing no toxicities at lower levels for both mice and nematodes. We analyzed mRNA data from infected nematodes to investigate how CRKP infection affects C. Elegans. We found that CRKP infection may activate the FoxO signaling pathway, weakening the antioxidant defense of nematodes and increasing mortality [41]. Therefore, ROS levels in nematodes contribute to mortality after infection, evidenced by altered ROS levels in deceased nematodes. Silver and copper ions at 10^{-2} M concentrations increased ROS levels in deceased nematodes. Therefore, ROS levels in nematodes contribute to mortality after infection. Silver and copper ions at 10^{-2} M concentrations also increased ROS levels in deceased nematodes. Previous studies suggested that antioxidants can prevent or delay damage by reducing ROS levels. This indicates that antioxidants may protect against metal ion toxicity and ROS-induced damage in the C. elegans model of CRKP infection. Antioxidants can mitigate metal ion toxicity caused by elevated ROS levels while maintaining the antibacterial properties of the metal ions. Previous studies suggested that antioxidants can help prevent or delay harmful processes by reducing ROS levels. This indicates that antioxidants may protect against metal ion toxicity and ROS-induced damage in the C. elegans model of CRKP infection [42]. In the future, this strategy can help develop antimicrobial agents. The role of the circulatory system and the blood-brain barrier were neglected in our study. Therefore, the C. elegans model can only play a preliminary role in infection and toxicity screening, and the

results need to be verified in mammalian experiments.

C. elegans lacks certain anatomical features, limiting its role in infection and toxicity screening. Further mammalian experiments are required to confirm these findings. Additionally, the potential of antioxidants to reduce metal ion toxicity and improve antibacterial activity needs more verification.

This model can be a new addition to develop antimicrobial agents, but our study has some limitations. C. elegans lacks certain anatomical features, and more studies are needed to confirm the potential of antioxidants in reducing metal ion toxicity and improving the antibacterial effects.

Conclusions

In conclusion, the *C. elegans* model can help assess the antibacterial properties and toxicity of metal ions, ameliorating metal ion toxicity while maintaining their antibacterial properties to resolve CRKP infection. The lethal mechanism underlying CRKP infection and metal ion toxicity may be associated with ROS overproduction. In future studies, antioxidants can be employed to mitigate metal ion toxicity, thereby offering a novel avenue for treating drug-resistant bacteria.

Acknowledgements

The current study was supported by grants from National Natural Science Foundation of China (Grant No. 82260597). Natural Science Foundation of Jiangxi Province (20202BAB206063, 009033469014). Science and Technology Bureau of Nanchang (Hongkezi [2021] 129), Science and Technology Bureau of Nanchang (Hongkezi [2021] 200), and Nanchang high-level scientific and technological innovation talent “Double hundred Plan” (Hongkezi [2023] 228). Jiangxi Science and Technology Plan of Health Commission (20204032).

Disclosure of conflict of interest

None.

Address correspondence to: Dr. Liping Li, Department of Clinical Laboratory, The Third Affiliated Hospital of Nanchang University (The First Hospital of Nanchang), Nanchang 330008, Jiangxi, P. R. China. Tel: +86-15179105426; E-mail: liliping-2012@hotmail.com

References

[1] Willyard C. The drug-resistant bacteria that pose the greatest health threats. Nature 2017; 543: 15.

[2] Shen H, Liu Y, Liu Y, Duan Z, Wu P, Lin Z and Sun H. Hormetic dose-responses for silver antibacterial compounds, quorum sensing inhibitors, and their binary mixtures on bacterial resistance of Escherichia coli. Sci Total Environ 2021; 786: 147464.

[3] Hassanen EI and Ragab E. In vivo and in vitro assessments of the antibacterial potential of chitosan-silver nanocomposite against methicillin-resistant staphylococcus aureus-induced infection in rats. Biol Trace Elem Res 2021; 199: 244-257.

[4] Ivanauskas R, Bronusiene A, Ivanauskas A, Šarkinas A and Ancutiene I. Antibacterial activity of copper particles embedded in knitted fabrics. Materials (Basel) 2022; 15: 7147.

[5] JankauskaitĽ V, VitkauskienĽ A, Lazauskas A, Baltrusaitis J, ProsyĽevas I and AndruleviĽius M. Bactericidal effect of graphene oxide/Cu/Ag nanoderivatives against Escherichia coli, Pseudomonas aeruginosa, Klebsiella pneumoniae, Staphylococcus aureus and Methicillin-resistant Staphylococcus aureus. Int J Pharm 2016; 511: 90-97.

[6] Burghardt I, Lüthen F, Prinz C, Kreikemeyer B, Zietz C, Neumann HG and Rychly J. A dual function of copper in designing regenerative implants. Biomaterials 2015; 44: 36-44.

[7] Lingscheid T, Tobudic S, Poeppl W, Mitteregger D and Burgmann H. In vitro activity of doripenem plus fosfomycin against drug-resistant clinical blood isolates. Pharmacology 2013; 91: 214-218.

[8] Arya S, Williams A, Reina SV, Knapp CW, Kreft JU, Hobman JL and Stekel DJ. Towards a general model for predicting minimal metal concentrations co-selecting for antibiotic resistance plasmids. Environ Pollut 2021; 275: 116602.

[9] Coley WC, Akhavi A, Sandu C, Pena PA, Lee I, Ozkan M and Ozkan CS. Copper-carbon hybrid nanoparticles as antimicrobial additives. MRS Commun 2022; 12: 1197-1203.

[10] Thneibat A, Fontana M, Cochran MA, Gonzalez-Cabezas C, Moore BK, Matis BA and Lund MR. Anticariogenic and antibacterial properties of a copper varnish using an in vitro microbial caries model. Oper Dent 2008; 33: 142-148.

[11] Tralau T, Riebeling C, Pirow R, Oelgeschläger M, Seiler A, Liebsch M and Luch A. Wind of

change challenges toxicological regulators. Environ Health Perspect 2012; 120: 1489-1494.
[12] Nass R and Hamza I. The nematode C. elegans as an animal model to explore toxicology in vivo: solid and axenic growth culture conditions and compound exposure parameters. Curr Protoc Toxicol 2007; Chapter 1: Unit1.9.
[13] Karmaus PWF and Karmaus AL. Challenges for integrating immunotoxicology into the twenty-first-century toxicology testing paradigm. Methods Mol Biol 2018; 1803: 385-396.
[14] Zhang J, Holdorf AD and Walhout AJ. C. elegans and its bacterial diet as a model for systems-level understanding of host-microbiota interactions. Curr Opin Biotechnol 2017; 46: 74-80.
[15] Hufnagel M, Schoch S, Wall J, Strauch BM and Hartwig A. Toxicity and gene expression profiling of copper- and titanium-based nanoparticles using air-liquid interface exposure. Chem Res Toxicol 2020; 33: 1237-1249.
[16] Beanan MJ and Strome S. Characterization of a germ-line proliferation mutation in C. elegans. Development 1992; 116: 755-766.
[17] Kim DH, Feinbaum R, Alloing G, Emerson FE, Garsin DA, Inoue H, Tanaka-Hino M, Hisamoto N, Matsumoto K, Tan MW and Ausubel FM. A conserved p38 MAP kinase pathway in Caenorhabditis elegans innate immunity. Science 2002; 297: 623-626.
[18] Ahn JM, Eom HJ, Yang X, Meyer JN and Choi J. Comparative toxicity of silver nanoparticles on oxidative stress and DNA damage in the nematode, Caenorhabditis elegans. Chemosphere 2014; 108: 343-352.
[19] Hackbarth H, Küppers N and Bohnet W. Euthanasia of rats with carbon dioxide--animal welfare aspects. Lab Anim 2000; 34: 91-96.
[20] Hadrup N, Loeschner K, Bergström A, Wilcks A, Gao X, Vogel U, Frandsen HL, Larsen EH, Lam HR and Mortensen A. Subacute oral toxicity investigation of nanoparticulate and ionic silver in rats. Arch Toxicol 2012; 86: 543-551.
[21] Diamandas A, Razon MR, Ramirez-Arcos S and Brassinga AKC. The virulence of S. marcescens strains isolated from contaminated blood products is divergent in the C. elegans infection model. Front Genet 2021; 12: 667062.
[22] Partridge FA, Brown AE, Buckingham SD, Willis NJ, Wynne GM, Forman R, Else KJ, Morrison AA, Matthews JB, Russell AJ, Lomas DA and Sattelle DB. An automated high-throughput system for phenotypic screening of chemical libraries on C. elegans and parasitic nematodes. Int J Parasitol Drugs Drug Resist 2018; 8: 8-21.
[23] Huang Q, Li R, Yi T, Cong F, Wang D, Deng Z and Zhao YL. Phosphorothioate-DNA bacterial diet reduces the ROS levels in C. elegans while improving locomotion and longevity. Commun Biol 2021; 4: 1335.
[24] Back P, Braeckman BP and Matthijssens F. ROS in aging Caenorhabditis elegans: damage or signaling? Oxid Med Cell Longev 2012; 2012: 608478.
[25] Zijno A, De Angelis I, De Berardis B, Andreoli C, Russo MT, Pietraforte D, Scorza G, Degan P, Ponti J, Rossi F and Barone F. Different mechanisms are involved in oxidative DNA damage and genotoxicity induction by ZnO and TiO2 nanoparticles in human colon carcinoma cells. Toxicol In Vitro 2015; 29: 1503-1512.
[26] Khanna P, Ong C, Bay BH and Baeg GH. Nanotoxicity: an interplay of oxidative stress, inflammation and cell death. Nanomaterials (Basel) 2015; 5: 1163-1180.
[27] Ratnasekhar Ch, Sonane M, Satish A and Mudiam MK. Metabolomics reveals the perturbations in the metabolome of Caenorhabditis elegans exposed to titanium dioxide nanoparticles. Nanotoxicology 2015; 9: 994-1004.
[28] Alexpandi R, Prasanth MI, Ravi AV, Balamurugan K, Durgadevi R, Srinivasan R, De Mesquita JF and Pandian SK. Protective effect of neglected plant Diplocyclos palmatus on quorum sensing mediated infection of Serratia marcescens and UV-A induced photoaging in model Caenorhabditis elegans. J Photochem Photobiol B 2019; 201: 111637.
[29] Thangamani S, Eldesouky HE, Mohammad H, Pascuzzi PE, Avramova L, Hazbun TR and Seleem MN. Ebselen exerts antifungal activity by regulating glutathione (GSH) and reactive oxygen species (ROS) production in fungal cells. Biochim Biophys Acta Gen Subj 2017; 1861: 3002-3010.
[30] Lipinski C and Hopkins A. Navigating chemical space for biology and medicine. Nature 2004; 432: 855-861.
[31] Projan SJ and Shlaes DM. Antibacterial drug discovery: is it all downhill from here? Clin Microbiol Infect 2004; 10 Suppl 4: 18-22.
[32] Phillips PC. Self-fertilization sweeps up variation in the worm genome. Nat Genet 2012; 44: 237-238.
[33] Peterson ND and Pukkila-Worley R. Caenorhabditis elegans in high-throughput screens for anti-infective compounds. Curr Opin Immunol 2018; 54: 59-65.
[34] Garsin DA, Sifri CD, Mylonakis E, Qin X, Singh KV, Murray BE, Calderwood SB and Ausubel FM. A simple model host for identifying Gram-positive virulence factors. Proc Natl Acad Sci U S A 2001; 98: 10892-10897.
[35] Mallo GV, Kurz CL, Couillault C, Pujol N, Granjeaud S, Kohara Y and Ewbank JJ. Inducible anti-

bacterial defense system in C. elegans. Curr Biol 2002; 12: 1209-1214.
[36] Conery AL, Larkins-Ford J, Ausubel FM and Kirienko NV. High-throughput screening for novel anti-infectives using a C. elegans pathogenesis model. Curr Protoc Chem Biol 2014; 6: 25-37.
[37] Lavigne JP, Cuzon G, Combescure C, Bourg G, Sotto A and Nordmann P. Virulence of Klebsiella pneumoniae isolates harboring bla KPC-2 carbapenemase gene in a Caenorhabditis elegans model. PLoS One 2013; 8: e67847.
[38] Ning C, Wang X, Li L, Zhu Y, Li M, Yu P, Zhou L, Zhou Z, Chen J, Tan G, Zhang Y, Wang Y and Mao C. Concentration ranges of antibacterial cations for showing the highest antibacterial efficacy but the least cytotoxicity against mammalian cells: implications for a new antibacterial mechanism. Chem Res Toxicol 2015; 28: 1815-1822.
[39] Romo Quiñonez CR, Alvarez-Ruiz P, Mejía-Ruiz CH, Bogdanchikova N, Pestryakov A, Gamez-Jimenez C, Valenzuela-Quiñonez W, Montoya-Mejía M and Nava Pérez E. Chronic toxicity of shrimp feed added with silver nanoparticles (Argovit-4®) in Litopenaeus vannamei and immune response to white spot syndrome virus infection. PeerJ 2022; 10: e14231.
[40] Gajda-Meissner Z, Matyja K, Brown DM, Hartl MGJ and Fernandes TF. Importance of surface coating to accumulation dynamics and acute toxicity of copper nanomaterials and dissolved copper in daphnia magna. Environ Toxicol Chem 2020; 39: 287-299.
[41] Zečić A and Braeckman BP. DAF-16/FoxO in Caenorhabditis elegans and its role in metabolic remodeling. Cells 2020; 9: 109.
[42] Zeitoun-Ghandour S, Leszczyszyn OI, Blindauer CA, Geier FM, Bundy JG and Stürzenbaum SR. C. elegans metallothioneins: response to and defence against ROS toxicity. Mol Biosyst 2011; 7: 2397-2406.